

# Experimenting Acceleration Feedback Loop for Robot Control

Pasquale Chiacchio<sup>°</sup> François Pierrot\* Bruno Siciliano<sup>°</sup>

<sup>°</sup>Dipartimento di Informatica e Sistemistica  
Università degli Studi di Napoli Federico II  
Via Claudio 21, 80125 Napoli, Italy  
E-mail: siciliano@vaxna1.na.infn.it

\*Laboratoire d'Informatique, de Robotique et de Microélectronique de Montpellier  
Université Montpellier II  
161 rue Ada, 34392 Montpellier Cedex 5, France

## Abstract

*The dynamic model of a robot manipulator is usually described by a set of nonlinear, highly coupled differential equations. However, linear control schemes (namely PD or PID independent joint controllers) are often used, the manipulator being regarded as a set of linear independent dynamic systems with the nonlinear and coupling effects acting as disturbances. These simple schemes cannot achieve good performance due to their inherent low rejection to disturbances. A way to overcome this problem without losing the simplicity of a linear controller is to use also acceleration information. This paper describes experiments intended to demonstrate that such a solution is feasible and effective. Using a transputer-based system we were able to reconstruct acceleration and velocity information from position measurements and control a high-speed parallel robot. The obtained results confirm the good performance of the control scheme which we believe can be a valid alternative to model-based control algorithms.*

**Keywords:** Robotics, Independent joint control, Linear control, Acceleration feedback, Disturbance rejection.

## 1. Introduction

In recent years, model-based controllers have received a growing attention from the robotics community. These controllers compensate for the available estimates of the dynamic terms in a feedforward or in a feedback fashion with linear feedback loops overcoming the effects of imperfect modeling and unavoidable disturbances [1,2]. They have also proved their effectiveness for manipulators with high gear ratios, for which is commonly accepted that nonlinear and coupling effects can be neglected [3,4].

There are two main disadvantages related to this kind of controllers. One is the necessity of a complex process to identify the actual terms of the dynamic model. The other is the difficulty to face problems arising from payload variations, variable friction coefficients and so on, so that adaptive control schemes have to be considered [5].

Another possible approach in robot control is to regard the manipulator as a set of linear decoupled dynamic subsystems with the nonlinear and coupling effects acting as disturbances. Following this approach, simple linear controllers can be designed; as a matter of fact most, if not all, industrial manipulators are controlled by means of independent PD or PID joint controllers. The obtained performance is obviously very poor if dynamics effects are not negligible (as when tracking of high-speed, high-acceleration trajectories is required) since such simple controllers cannot reject the effect of these disturbances.

A possible way to achieve better performance, still retaining the simplicity of linear independent joint control, is to use also acceleration information in the feedback. In a recent paper [6], this problem has been addressed and a state variable filter has been presented to reconstruct the acceleration—and eventually the velocity—from position measurements. The proposed controller required very short sampling times and only simulations were provided showing that it is possible to effectively use this method within the constraints imposed by available computers.

In this paper we show that such a controller has good performance also in a real experimental setup. We have implemented it on a multi-transputer system controlling a high-speed parallel robot. Experimental results are presented. The controller has been tested at different sampling times and compared with a classical PID controller.

The paper is organized as follows. Section 2 gives the basic theory on the design of the controller. In Section 3 we describe the experimental setup. The results are presented and commented in Section 4. Conclusions are drawn in Section 5.

## 2. Controller design

The dynamic equations of an  $n$  degree-of-freedom manipulator in free space can be written as

$$(B_c + B_v(q))\ddot{q} + C(q, \dot{q})\dot{q} + F\dot{q} + g(q) = \tau \quad (1)$$

where  $q$  is the  $(n \times 1)$  vector of joint variables,  $B_c$  is the  $(n \times n)$  constant diagonal matrix whose elements

are the average values of joint inertias, with  $B_v$  being the remaining part of the positive definite symmetric inertia matrix,  $C\dot{q}$  is the  $(n \times 1)$  vector of Coriolis and centrifugal forces,  $F\dot{q}$  is the  $(n \times 1)$  vector of joint friction forces,  $g$  is the  $(n \times 1)$  vector of gravitational forces, and  $\tau$  is the  $(n \times 1)$  vector of joint driving forces. In a gear-driven manipulator, the joint driving forces are provided by the actuators via kinematic transmissions. This leads to the relation

$$K_r q = q_m \quad (2)$$

where  $q_m$  is the  $(n \times 1)$  vector of actuator displacements, and  $K_r$  is an  $(n \times n)$  diagonal matrix whose elements are greater than unity. The  $(n \times 1)$  vectors of actuator driving forces  $\tau_m$  is given by

$$\tau_m = I_m \ddot{q}_m + F_m \dot{q}_m + K_r^{-1} \tau \quad (3)$$

where  $I_m$  and  $F_m$  are  $(n \times n)$  diagonal matrices whose elements are the inertia and the viscous friction coefficients of the motors plus the transmissions, and  $\tau$  is given by (1).

Plugging (1) into (3) gives

$$\tau_m = (I_m + K_r^{-1} B_c K_r^{-1}) \ddot{q}_m + (F_m + K_r^{-1} F K_r^{-1}) \dot{q}_m + \tau_{NL} \quad (4)$$

where

$$\tau_{NL} = K_r^{-1} B_v K_r^{-1} \ddot{q}_m + K_r^{-1} C K_r^{-1} \dot{q}_m + K_r^{-1} g. \quad (5)$$

From (4) it is clear that the manipulator can be regarded as a set of independent linear dynamic systems, with the nonlinear and coupling terms given in (5) acting as disturbances. It is understood that  $\tau_{NL}$  can include also any model uncertainty of system components.

The simplified model for an actuated joint is described by the voltage-to-position second-order transfer function

$$G(s) = \frac{k_m}{s(1 + s\tau_m)} \quad (6)$$

where  $k_m$  and  $\tau_m$  depends on the parameters in eq. (4) and on the particular actuator used.

A classical joint controller (hereafter called P-PI) which operates only on position and velocity information is shown in Fig. 1.

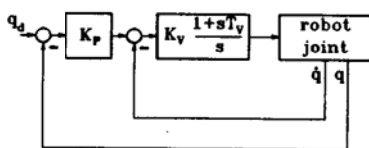


Fig. 1. P-PI controller

With this controller, assuming the joint dynamics is described by (6) and choosing  $T_v = \tau_m$ , the resulting input/output transfer function can be written in the classical form

$$W(s) = \frac{1}{1 + \frac{2\zeta}{\omega_n} s + \frac{s^2}{\omega_n^2}} \quad (7)$$

If the natural frequency  $\omega_n$  (related to the bandwidth) and the damping ratio  $\zeta$  (related to the overshoot) are given as design requirements, the controller gains  $K_P$  and  $K_V$  can be obtained from the relations

$$K_V = \frac{2\zeta\omega_n}{k_m} \quad (8)$$

$$K_P K_V = \frac{\omega_n^2}{k_m} \quad (9)$$

Obviously, since an integrator term is present in the controller, the system has zero error at steady-state when a step disturbance occurs. A measure of the disturbance rejection factor during the transient is given by

$$X_R = K_P K_V. \quad (10)$$

It must be remarked, moreover, that if the joint controller is required to follow a high-speed trajectory, the tracking capabilities of the scheme can be improved by feedforward cancellation of the motor dynamics. In particular, the input of the P-PI scheme can be modified into

$$\left(1 + \frac{s}{K_P} + \frac{s^2}{k_m K_P K_V}\right) Q_d(s) \quad (11)$$

resulting into a zero tracking error.

The reader is referred to [6] for further details on the derivation of this and the following controller.

In order to allow the setting of desired values for the disturbance rejection factor, the addition of an acceleration feedback loop has been proposed in the P-P-PI controller drawn in Fig. 2 assuming that acceleration measurements are available.

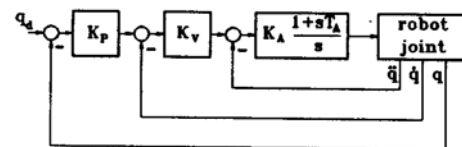


Fig. 2. P-P-PI controller

Again, by choosing  $T_A = \tau_m$ , one obtains the same closed-loop transfer function as in (7). We can compute the gains  $K_P$ ,  $K_V$  and  $K_A$  from the relations

$$2K_P = \frac{\omega_n}{\zeta} \quad (12)$$

$$1 + k_m K_A = \frac{k_m X_R}{\omega_n^2} \quad (13)$$

$$K_P K_V K_A = X_R. \quad (14)$$

Now the disturbance rejection factor  $X_R$  can be a further design requirement instead of being fixed when  $\omega_n$  and  $\zeta$  are given as for the P-PI controller.

Perfect tracking can be achieved by a feedforward compensation action, i.e. modifying the input as

$$\left(1 + \frac{s}{K_P} + \frac{(1 + k_m K_A)s^2}{k_m K_P K_V K_A}\right) Q_d(s). \quad (15)$$

The main problem of the P-P-PI controller of Fig. 2 is direct measurements of acceleration which in general are either not available or too expensive to get. However, it is possible to reconstruct the joint acceleration (and eventually velocity too) using a state variable filter whose input is the joint position measurement.

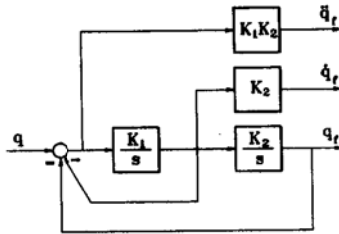


Fig. 3. State variable filter

The filter (Fig. 3) is characterized by a natural frequency  $\omega_{nf} = \sqrt{k_1 k_2}$  and by a damping ratio  $\zeta_f = \frac{1}{2} \sqrt{\frac{k_1}{k_2}}$ . Choosing filter bandwidth to be larger than joint servo bandwidth—at least a decade off to the right—good reconstruction of velocity and acceleration can be obtained.

### 3. Experimental setup

In order to test the practical implementation of the proposed P-P-PI controller, the high-speed three-degree-of-freedom parallel robot DELTA [7] available at LIRMM was considered (Fig. 4).

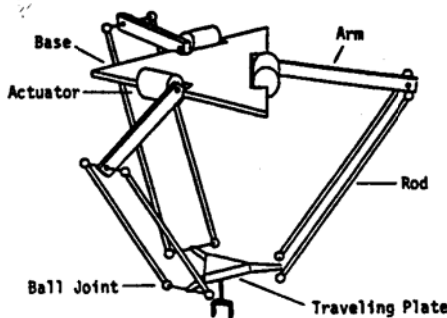


Fig. 4. DELTA robot

This robot has a traveling plate connected to the base plate by three kinematic chains actuated by PARVEX brushless motors. Each motor is equipped with a digital encoder whose resolution is 10000 counts per revolution. It was exploited the possibility, offered by the motors' amplifiers, of controlling the currents. Even if the robot is very light, the nonlinear and coupling dynamical terms cannot be considered negligible [8]; this is due also to the fact that, in the laboratory prototype, the gear ratio is only 1:10.

A very fast three-Transputer system of INMOS T800's was utilized, whose boards were developed at LIRMM (Fig. 5). One of the boards is used to implement the control algorithms and communicate with the host PC; the decoding of joint encoders' measurements plus the reconstruction of both joint velocity and acceleration are performed on another transputer board; the third board is basically a D/A output board.

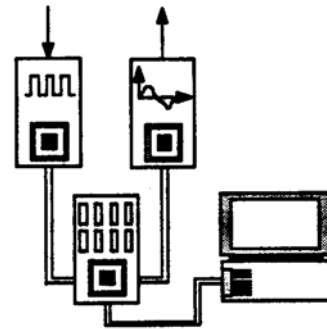


Fig. 5. Transputer system layout

A rough identification process was performed; with only the arm connected to the motor via the gear transmission, the identified parameters of the linear model in (5) are  $k_m = 837.7 \text{ sec/V}$  and  $T_m = 0.4 \text{ sec}$ . Also, the presence of a static friction torque of 0.05 Nm was identified.

The design specs for the P-PI controller were  $\omega_n = 62.8 \text{ rad/sec}$  and  $\zeta = 0.7$ ; the gains were computed via (8,9), resulting in a disturbance rejection factor  $X_R = 4.7$ . On the other hand, different values of  $X_R$  were set for the P-P-PI controller and the relative gains were computed via (12-14). As for the state-variable filter used to reconstruct velocity and acceleration,  $\omega_{nf} = 628 \text{ rad/sec}$  and  $\zeta = 0.5$  were chosen to ensure good reconstruction. Both the controllers and the reconstructing filter were converted in their discrete-time equivalent versions before implementation.

### 4. Experimental results

Two sets of experimental tests were performed. In the first set, only one motor with its arm connected via the gear transmission is controlled so that no dynamic coupling is present; the same conditions as for the identification process hold. In the second set, the whole robot

was employed and the same controller for one motor with the same gains as above were used while the other motors are not controlled; this allows to evaluate the capability of rejecting the disturbance caused by dynamic coupling.

First, the two control schemes (P-PI and P-P-PI) were compared at a sampling time of 0.3 msec. For each test the following schemes were used: without feedforward (labelled 1 in the figures), with feedforward of static friction (label 2), with feedforward of velocity and velocity+acceleration (eqs. (11) and (15) — label 3), with both feedforward actions (label 4). In all trials, the same motor was moved of 5000 encoder counts using a fifth-order polynomial as the reference trajectory (dashed line in the figures); the motor starts and arrives at rest, and it reaches one half of the maximum allowable velocity and acceleration. This corresponds to a joint motion of 0.314 rad to be performed in 0.075 sec, with a maximum velocity of 8 rad/sec and a maximum acceleration of 340 rad/sec<sup>2</sup>; at the arm tip the resulting maximum velocity is of 2 m/sec and the maximum acceleration of 88 m/sec<sup>2</sup> ( $\approx 9g$ ).

Figure 6 shows the obtained trajectories and tracking errors when the P-PI controller was used and only the arm was connected. Notice that the use of feedforward terms gives better results, since the system is in the same condition under which identification was carried out. In Figure 7 the same curves are plotted when the whole robot is running; it is quite evident to recognize the poor performance of the scheme. The errors are given in encoder counts; 100 counts correspond to 0.00628 rad at the joint.

Next, the P-P-PI controller was applied under the same conditions. The disturbance rejection factor was  $X_R = 10$ ; larger values lead to gains causing instability. In Figures 8 and 9 the errors are plotted for the single arm and the whole robot, respectively. It is clear that this scheme performs better than the P-PI scheme; the errors in both cases are as much as half of the previous ones — the rejection factor is now almost doubled.

In order to obtain higher disturbance rejection factors with the P-P-PI controller while preserving closed-loop system stability, it is necessary to decrease the sampling time. With a sampling time of 0.2 msec, it was possible to achieve  $X_R = 15$ . Figure 10 shows that tracking errors for the whole robot become smaller. Further, with a sampling time of 0.16 msec, which is the minimum achievable with the transputer system, it was obtained  $X_R = 18$ . The resulting errors for the whole robot are plotted in Fig. 11. In this case, it is worth noticing that there is no substantial difference on the tracking performance when feedforward is added; in fact, with such a rejection factor, the P-P-PI controller does not need an accurate knowledge of the model. Nevertheless, it should be recalled that the feedforward actions are based only on a rough identification of the linearized model and of the static friction torque.

## 5. Conclusions

Experiments on the use of acceleration feedback in the control of a high speed parallel robot have been described in this paper. The acceleration (and velocity) information is computed from the position measurement via a state variable filter. The controller has been implemented on a transputer-based system. The obtained results have confirmed the theoretical findings, i.e. closing an extra feedback loop around the disturbance input achieves better performance over the conventional PID scheme in terms of disturbance rejection factor. In conclusion, it is believed that the proposed control scheme represents a practical, valid alternative to model-based control schemes of second-order mechanical systems with highly coupled dynamics.

## Acknowledgements

This work was partly supported by Commission of the European Communities under an ESPRIT Research Grant assigned to the first author to support his stay at LIRMM in Montpellier and by Consiglio Nazionale delle Ricerche under contract no. 92.01064.PF67.

## References

- [1] J.Y.S. Luh, M.W. Walker, and R.C.P. Paul, "Resolved-acceleration control of mechanical manipulators," *IEEE Trans. on Automatic Control*, vol. 25, pp. 468-474, 1980.
- [2] C.H. An, C.G. Atkenson, and J.M. Hollerbach, *Model-Based Control of Robot Manipulators*, MIT Press, Cambridge, MA, 1988.
- [3] M.B. Leahy Jr. and G.N. Saridis, "Compensation of industrial manipulator dynamics," *Int. J. of Robotics Research*, vol. 8, no. 4, pp. 73-84, 1989.
- [4] P. Chiacchio, L. Sciavicco, and B. Siciliano, "The potential of model-based control algorithms for improving industrial robot tracking performance," *Proc. of IEEE Int. Work. on Intelligent Motion Control*, Istanbul, TR, pp. 831-836, 1990.
- [5] J.-J.E. Slotine and W. Li, "On the adaptive control for robot manipulators," *Int. J. of Robotics Research*, vol. 6, no. 3, pp. 49-59, 1987.
- [6] P. Chiacchio, L. Sciavicco, and B. Siciliano, "Practical design of independent joint controllers for industrial robot manipulators," *Proc. 1992 American Control Conf.*, Chicago, IL, pp. 1239-1240, 1992.
- [7] F. Pierrot, C. Reynaud, and A. Fournier, "DELTA: A simple and efficient parallel robot," *Robotica*, vol. 8, pp. 105-109, 1990.
- [8] F. Pierrot, A. Fournier, and P. Dauchez, "Towards a fully-parallel 6 dof robot for high speed applications," *Proc. 1991 IEEE Int. Conf. on Robotics and Automation*, Sacramento, CA, pp. 1288-1293, 1991.

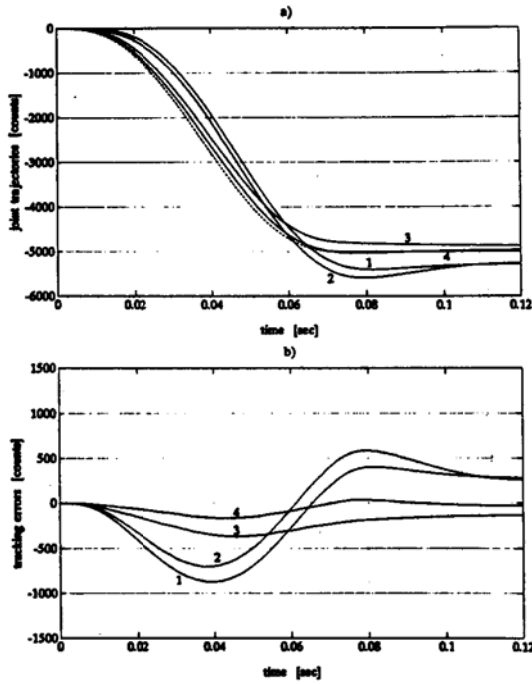


Fig. 6. P-PI scheme for the sole arm at a sampling time of 0.3 msec: a) time history of desired and actual joint trajectories, b) time history of tracking errors

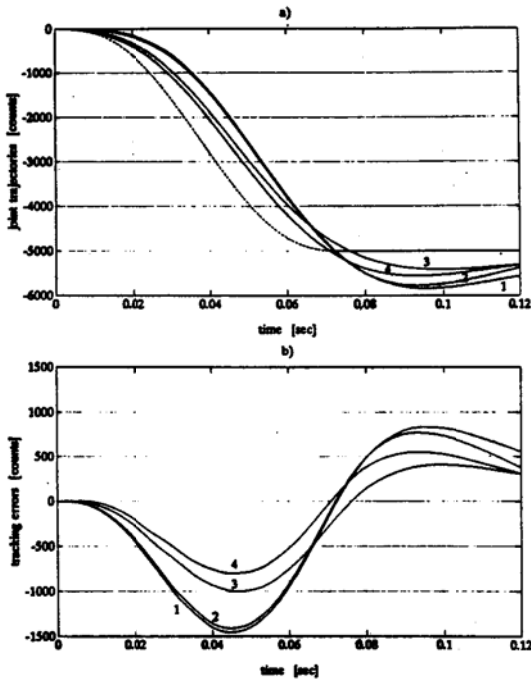


Fig. 7. P-PI scheme for the whole robot at a sampling time of 0.3 msec: a) time history of desired and actual joint trajectories, b) time history of tracking errors

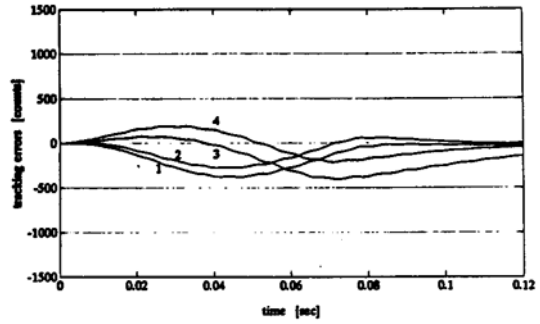


Fig. 8. Time history of tracking errors with the P-P-PI scheme for the sole arm at a sampling time of 0.3 msec

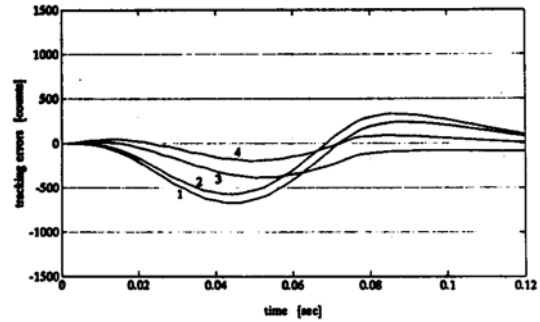


Fig. 9. Time history of tracking errors with the P-P-PI scheme for the whole robot at a sampling time of 0.3 msec

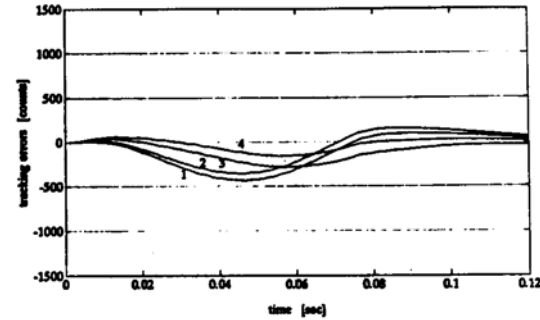


Fig. 10. Time history of tracking errors with the P-P-PI scheme for the whole robot at a sampling time of 0.2 msec

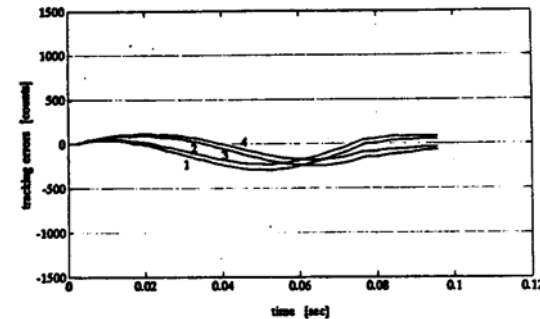


Fig. 11. Time history of tracking errors with the P-P-PI scheme for the whole robot at a sampling time of 0.16 msec

# Shortest path synthesis for a car-like robot\*

Philippe Souères  
soueres@laas.fr

Jean-Paul Laumond  
jpl@laas.fr

LAAS/CNRS, 7 Avenue du Colonel Roche  
31077 Toulouse, France

**Abstract :** This paper deals the characterization of shortest paths for a non-holonomic mobile robot constrained to move with a minimal turning radius. We provide the partition of the configuration space induced by the shape of the shortest paths reaching the origin. This work completes the results obtained by Reeds and Shepp [8], and more recently, by Sussmann *et al* [11] and Boissonnat *et al* [1].

**Keywords :** Optimal Trajectory Synthesis, Optimal Control, Nonholonomic Mobile Robot.

## 1 Introduction

A car-like robot is defined as the following control system :

$$\begin{pmatrix} \dot{x} \\ \dot{y} \\ \dot{\theta} \end{pmatrix} = \begin{pmatrix} \cos \theta & 0 \\ \sin \theta & 0 \\ 0 & 1 \end{pmatrix} \begin{pmatrix} \omega_1 \\ \omega_2 \end{pmatrix} \quad (1)$$

with

$$|\omega_1(t)| \leq 1 \quad \text{and} \quad |\omega_2(t)| \leq 1 \quad (2)$$

$(x, y) \in \mathbf{R}^2$  are the coordinates of the robot position, while  $\theta \in S^1$  is the direction of the robot. This system is an approximated model of a car moving forward and backward with a lower bounded turning radius and an upper bounded velocity. The minimum turning radius and the maximum velocity are assumed to be 1.

The problem of characterizing the shortest paths was first addressed by Dubins [4]. He proves the existence of shortest paths when  $\omega_1 = 1$  (i.e. the robot moves only forward with a constant velocity). He provides a sufficient family of simple paths which are sequences of at most 3 pieces consisting of straight line segments or arcs of circles of radius 1. This family always contains a shortest path.

In [3], Cockayne and Hall provide the classes of Dubins's paths by which the system can reach a given point and obtain the set of all the positions reachable at fixed time.

Reeds and Shepp extend Dubins's result to a system moving forward and backward with a constant velocity (i.e.  $|\omega_1| = 1$ ) [6]. They prove that a shortest path can always be chosen among 48 simple paths constituted by

some sequences of at most 5 pieces which are straight line segments or arcs of circle of radius 1. Such simple paths contain at most 2 cusps.

All these studies have been done without any reference to the optimal control theory. More recently, Sussmann *et al* [9] and Boissonnat *et al* [1] independently give a new proof of Reeds and Shepp's result by using the maximum principle. Such new proofs refine the previous result. Sussmann *et al* reduce to 46 the number of the potentially shortest paths. Moreover they prove that the solutions for the system (1) with  $|\omega_1| = 1$  hold when  $|\omega_1| \leq 1$ .

In this paper, we complete the study by providing the partition of  $\mathbf{R}^2 \times S^1$  induced by the shape of the shortest paths reaching the origin. This partition provides a way to compute a synthesis of the shortest paths. Moreover, we derive the sets of points where the shortest paths are not unique, and, among them, the sets of points of discontinuity (i.e. the cut-locus of the system).

The study is based on the following method :

- 1/ We first prove symmetry properties in each plane  $P_\theta$  corresponding to constant value of  $\theta$ . These results allow us to restrict our study to one quadrant bounded by two symmetry axes in  $P_\theta$  (Section 3.1). Then we prove that we only have to consider the value of  $\theta$  in  $[-\pi, \pi]$  (Section 3.2).
- 2/ We compute all the domains in  $P_\theta$  corresponding to the starting point of each type of path in Reeds and Shepp's family refined by the symmetry properties. We parametrize the paths by two real numbers whose variations induce a foliation of each domain.
- 3/ We reduce these domains by using symmetry properties and direct geometric arguments combined with the necessary conditions provided by the maximum principle (Section 5).
- 4/ At this point, almost all the domains are adjacent. Only two overlapping domains require a specific study (Section 6).

In our reasoning, we restrict the study to planes  $P_\theta$  corresponding to constant directions of the robot. In Section 7, we precise the values of  $\theta$  for which each domain exists.

**Notations :** We use the notations introduced by Reeds and Shepp and revised by Sussmann and Tang. A path is

\*This work is supported by the ECC Esprit 3 Program (Project 6546 PROMotion).